Deep-inelastic structure function of the pion in the null-plane phenomenology

T. Frederico
Instituto de Estudos Avançados, Centro Técnico Aeroespacial, 12.225 São José dos Campos, São Paulo, Brasil

G. A. Miller
Department of Physics FM-15, University of Washington, Seattle, Washington 98195
(Received 29 October 1992)

The null-plane pion wave function is used to compute the structure function for deep-inelastic unpolarized-lepton scattering. The old problems with such a phenomenology are that the computed structure functions are almost independent of the Bjorken x variable, and that it is difficult to simultaneously reproduce the observed charge radius and pion decay constant. These are avoided by using constituent quarks with structure.

PACS number(s): 14.40.Aq, 12.39.Pn, 13.40.Gp, 13.60.Hb

I. INTRODUCTION

The wave function defined on the null plane [using $(x^0 + x^3 = 0)$ as the "time" coordinate] allows a relativistic description of two-body bound states with two important simplifications: (i) the center-of-mass (c.m.) coordinate is easily separated [1,2] and (ii) pair creation diagrams disappear for some processes [1,3].

One can obtain the null-plane wave function from the relevant quark diagram by performing the integration over the null-plane "time" or "energy." For example, in the evaluation of the pion form factor and weak decay constant from the quark-triangle diagram [3,4], the integration on $k^-(= k^0 - k^3)$ in the loop integral allows the identification of the null-plane wave function. Furthermore, computing the matrix element of the so-called "good" component of the electromagnetic current [5] $J^+(= J^0 + J^3)$ eliminates the effects of quark pair creation. We also note that our quark diagram approach yields the same formal results as the Hamiltonian front-form dynamics [6–8] as well as those of the earlier formalisms [1,2].

Here we study the quark-box diagram for the pion deep-inelastic scattering process. The integration over k^- in the momentum loop in the evaluation of the good component of the structure tensor allows the introduction of the null-plane $q\bar{q}$ pion bound state. The resulting structure function again turns out to be the same as that obtained in the Hamiltonian front form of the dynamics [9]. However, this pion structure function is essentially independent of the Bjorken x variable [2]. This problem is closely related to another old deficiency of constituent quark models, that of reproducing the observed values of the weak decay constant f_π and the mean charge radius r_π.

The purpose of this paper is to show that the problems involving the structure function, r_π and f_π can all be handled by treating the model of Ref. [4] more precisely. In that model [4] the quarks are constituent, with mass M obtained from the spontaneous breaking of chiral symmetry. Thus we expect that the constituent quark (or antiquark) has a nontrivial structure which should play a role in computing observables. In particular, each constituent object consists of a current quark surrounded by a cloud of partons. We make the simplifying assumptions that the cloud is locally neutral in both color and electric charge. However, the cloud does carry a significant fraction $1 - \eta$ (calculations below show $\eta \approx 0.5$) of the momentum of the quark. Including these features in different wave functions [4,6,13] leads to good agreement with the observed structure functions f_π and r_π. The notion that the pion is more than a simple pair of current quarks is consistent with the expectations about quantum chromodynamics (QCD) [10–12].

The plan of the paper is as follows. In Sec. II we review the formulation of the box diagram for the pion deep-inelastic structure function including non-$q\bar{q}$ components and also give the elastic form factor. In Sec. III, the numerical results for the valence deep-inelastic structure function for different models in the null plane are presented and compared. Section IV contains a brief summary.

II. STRUCTURE FUNCTION AND ELASTIC FORM FACTOR

The pion structure tensor $W^{\mu\nu}$ for inclusive electron scattering is the square of the modulus of the amplitude for the photon absorption summed over the parton phase space. For unpolarized electron scattering, it is written in terms of two invariants W_1 and W_2, according to current and parity conservation:

$$W^{\mu\nu} = W_1(x)\left[\frac{q^\mu q^\nu}{q^2} - g^{\mu\nu}\right] + \frac{W_2(x)}{m_\pi^2}\left[p^\mu - \frac{p\cdot q q^\mu}{q^2}\right]\left[p^\nu - \frac{p\cdot q q^\nu}{q^2}\right]. \quad (1)$$

In the laboratory frame $p^0 = m_\pi$(pion mass) and $\mathbf{p} = 0$. In the deep-inelastic limit $q^-(= q^0 - q^3) \to \infty$, and the results may be expressed in terms of the Bjorken variable x with $x = \frac{q^2}{2m_\pi q^0} = \frac{q^+}{m_\pi}$. In the parton model W_1 and W_2 are related by $W_2 = 2m_\pi^2 \frac{x}{p.q} W_1$.

The pion deep-inelastic structure function is calculated from the box diagram in Fig. 1(a). In the null-plane phenomenology the electromagnetic form factor is obtained from the triangle diagram [3,4] of Fig. 1(b) and f_π from the one-loop diagram [4] in Fig. 1(c). The PCAC (partial conservation of the axial vector current) relates the divergence of the matrix element of the axial vector current between the vacuum and pion states to the pion decay constant [15]. The diagram in Fig. 1(c) represents the above-mentioned matrix element of the axial vector current. The vertex for the process $\pi \to \bar{q}q \quad (= \frac{M}{f_\pi}\bar{q}\gamma^5 \boldsymbol{\tau} q)$ is determined by spontaneous breaking of the chiral symmetry, M is the constituent quark mass, and $\boldsymbol{\tau}$ are the isospin matrices. The nonpointlike nature of the pion is included [4] by modifying this vertex function, which can in principle be obtained by solving a Bethe-Salpeter equation. There is no pointlike pion in the model.

The utility of working with the effective Lagrangian for the pion quark coupling is twofold: (i) this scheme provides the correct quantum numbers for the composite pion and (ii) in our approach we use Feynman diagrams for the deep-inelastic process, f_π and r_π. Alternatively, one can construct the null-plane pion wave function as in Refs. [6,16,17], or work directly with QCD.

The details of the calculation of the structure tensor are given in the Appendix with the result

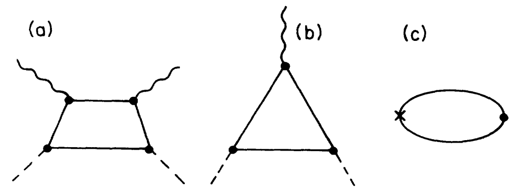

FIG. 1. One-loop quark diagrams for the valence structure function (a), electromagnetic form factor (b), and the pion decay constant (c).

$$W^{\mu\nu} = \mathrm{Im}\left\{2N_c e^2 \frac{5}{9}\frac{M^2}{f_\pi^2}\int \frac{d^4k}{(2\pi)^4}\delta(k^+ - p_\pi^+ + q^+)S^{\mu+\nu\sigma} \times \frac{\mathrm{tr}(-\not{k} + M)(\not{k} - \not{p}_\pi + M)\gamma_\sigma(\not{k} - \not{p}_\pi + M)}{(k^2 - M^2 + i\epsilon)[(k-p_\pi)^2 - M^2 + i\epsilon]^2}\right\}, \tag{2}$$

where e is the unit of charge, N_c the number of colors (3), q^μ is the photon momentum, p_π^μ is the pion initial momentum, k^μ is the momentum of the spectator quark. The conventions are given by Bjorken and Drell [18].

In order to relate Eq. (2) with the electromagnetic form factor calculated from J^+ we use $\mu = \nu = i$, with $i = 1$ or 2 as the transverse direction, $S^{i+i\sigma} = g^{i+}g^{i\sigma} + g^{i\sigma}g^{i+} - g^{ii}g^{+\sigma}$, from $g^{i+} = g^{i-} = 0$ results $\sigma = -$, and from $g^{+-} = \frac{1}{2}$ follow $S^{i+i-} = \frac{1}{2}$. Using $\gamma_- = \gamma^+$ in Eq. (2),

$$W^{ii} = \mathrm{Im}\left\{N_c e^2 \frac{5}{9}\frac{M^2}{f_\pi^2}\int \frac{d^4k}{(2\pi)^4}\delta(k^+ - p_\pi^+ + q^+)\frac{\mathrm{tr}(-\not{k} + M)(\not{k} - \not{p}_\pi + M)\gamma^+(\not{k} - \not{p}_\pi + M)}{(k^2 - M^2 + i\epsilon)[(k-p_\pi)^2 - M^2 + i\epsilon]^2}\right\}. \tag{3}$$

The next step is to obtain the structure function $F_1(x)$. We start by relating the transverse component of $W^{\mu\nu}$ to the structure function using Eq. (1) and deep-inelastic limit. Then

$$W^{ii} = W_1(x) \equiv \frac{5}{9}F_1(x). \tag{4}$$

This is obtained by doing the integration over k^- in Eq. (3). The result is

$$F_1(x) = \frac{2}{(2\pi)^3}\frac{M^2}{f_\pi^2}N_c \int \frac{d^2k_\perp}{x(1-x)}M_0^2 \frac{1}{(-m_\pi^2 + M_0^2)\,(-m_\pi^2 + M_0^2)}, \tag{5}$$

where

$$M_0^2(x, \mathbf{k}_\perp) = \frac{k_\perp^2 + M^2}{x(1-x)}.$$

Equation (5) also gives the normalization of the elastic form factor (see Eq. (8) of Ref. [4]) after the integration over x,

$$F_{\mathrm{el}}(q^2 = 0) = \int_0^1 dx\ F_1(x), \tag{6}$$

implying the sum rule $\int_0^1 F_1(x)dx = 1$, which is the statement that the charge of the π^+ is unity.

The pion wave function is introduced as in Ref. [4]:

$$\frac{1}{\pi^{\frac{3}{2}}}\frac{M}{f_\pi}\frac{\sqrt{M_0 N_c}}{-m_\pi^2 + M_0^2} \to \Phi_\pi(x, \mathbf{k}_\perp), \tag{7}$$

where $\mathbf{k}_\perp$ is the transverse relative momentum. Then $F_1(x)$ and F_{el} can be expressed, in the usual way, as integrals involving Φ_π. For example, the result for the structure function is obtained by replacing the mass denominator by the bound-state wave function in Eq. (5):

$$F_1(x) = \frac{1}{4}\int \frac{d^2k_\perp}{x(1-x)} M_0 \Phi_\pi^2(x,\mathbf{k}_\perp) \; . \tag{8}$$

The replacement (7) and subsequent modifications result from the assumption that the null-plane wave function is independent of k^-. Equation (8) is the same as the one deduced in the context of the Hamiltonian front form of the dynamics [9].

We also choose a phenomenological wave function by starting with different nonrelativistic ones that depend on $\mathbf{k}^2$. Here the third component of the momentum is given in terms of x and $\mathbf{k}_\perp$ by [6]

$$k_z = \left(x - \frac{1}{2}\right)\sqrt{\frac{k_\perp^2 + M^2}{x(1-x)}}. \tag{9}$$

This procedure amounts to a series of reasonable (but naive) guesses about what the solution to a relativistic theory involving confining interactions might look like.

However, the approach so far does not include the composite nature of the quark itself. We imagine the constituent quark to consist of a current quark surrounded by a cloud of partons that is locally colorless and electrically neutral. But the cloud contains some of the (+) momentum of the constituent quark. Then the valence structure function is a convolution

$$q^v(x) = \int_x^1 \frac{dy}{y} P(y) F_{q\bar{q}}\left(\frac{x}{y}\right) \; , \tag{10}$$

where $P(y)$ is the momentum distribution of the valence current quark component of the constituent quark and $F_{q\bar{q}}(x)$ is the structure function of the bound constituent quark in the pion. We assume that $F_{q\bar{q}}(x) = F_1(x)$ is given by Eq. (8).

The momentum distribution $P(x)$ must be of the general form

$$P(x) = \eta\delta(1-x) + \hat{P}(x), \tag{11}$$

with

$$\int_0^1 dx \hat{P}(x) = 1 - \eta. \tag{12}$$

The value of η gives the probability of the valence quark in the constituent quark. We shall choose η for each model wave function by requiring that the computed value of the decay constant reproduce the measured value. The function $\hat{P}$ accounts for the sharing of momentum between the current quark and the cloud; we need to model this quantity. As a simple choice reflecting our ignorance about the probability distribution of the recoil partons, we use

$$\hat{P}(x) = 1 - \eta \; , \tag{13}$$

which is fixed once η is determined. We do not introduce any other freedom in the model.

At this stage, we investigate the differences between the structure functions calculated with Eq. (8) and Eq. (10), for the same model of the $q\bar{q}$ component of the pion wave function. As an example, the result for the hydrogen-atom wave function, $\Phi_\pi(\mathbf{k}) \propto \frac{1}{[r_{NR}^{-2}+(\mathbf{k})^2]^2}$, using Eq. (8) is shown in Fig. 2. We chose $M = 220$ MeV and a nonrelativistic pion charge radius ($r_{\rm nr}$) of 0.195 fm. Both M and r_π come from the model of Ref. [13]. It is worthwhile to mention that in Ref. [13], the pion wave function is obtained from a dynamical calculation where the quark-antiquark potential has one-gluon exchange and confinement. But the form of the Φ_π can be well approximated by the dipole expression given above. We

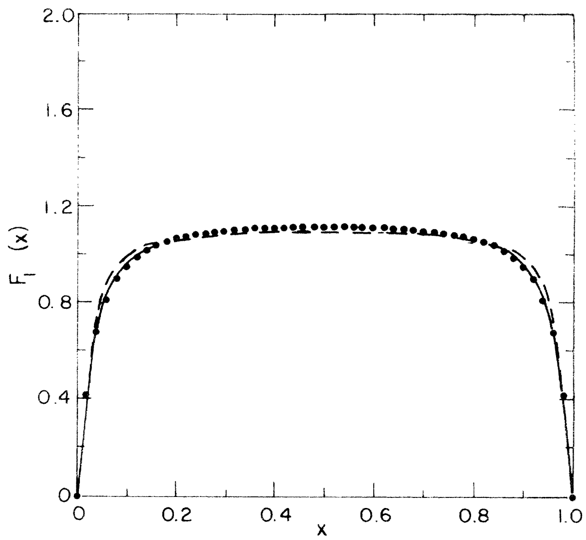

FIG. 2. Valence quark structure function of the pion [see Eq. (8)]. Constituent quark mass of 220 MeV. Hydrogen-atom model (solid line), Gaussian model (dashed line), and Ref. [13] (dotted line).

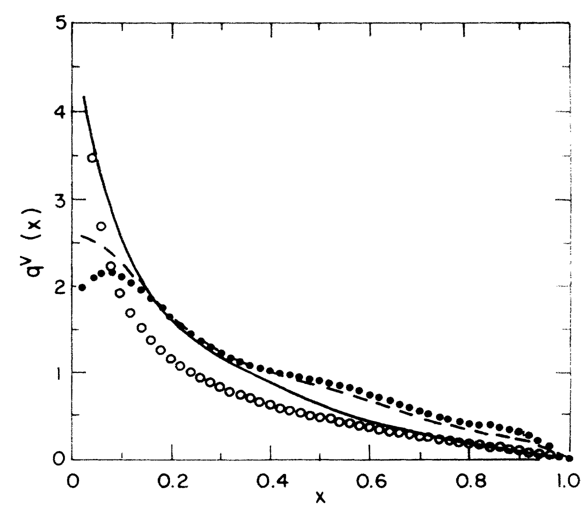

FIG. 3. First-order QCD evolution of the valence quark structure function of the pion. Hydrogen-atom model with $M=$ 300 MeV. Pion momentum scale, $Q_\pi=$ 0.5 GeV (solid line), 1 GeV (dashed line), and 1.5 GeV (dotted line). Distribution function of Ref. [21] at the momentum transfer of 2 GeV (circles).

observe that Eq. (8) yields an almost flat structure function with values around 1 except at the extremes where it vanishes. The results are about the same, if ones uses the Gaussian model, $\Phi_\pi(\mathbf{k}) = e^{-4/3(r_{NR}\mathbf{k})^2}$, with the above nonrelativistic radius and M or the model of Ref. [13]. Thus, the behavior of $F_1(x)$ does not depend on the details of the nonrelativistic wave function. Indeed, we can easily anticipate such behavior by analyzing Eq. (5). In the limit where $m_\pi = 0$, the structure function does not depend on x. This is strongly modified only at the edges for x near 1 and 0, when using a model wave function. These features are clear in Fig. 2.

On the other hand, using Eq. (10) leads to a valence structure function that peaks at small x (see Fig. 3). This is the trend of the experimental data, as discussed in the next section.

This more precise treatment of our model requires us to reexamine our earlier [4] results for the pion electromagnetic form factor $F_{\rm el}$. In our present treatment, the cloud carries no charge density. In that case, the computation of $F_{\rm el}$ is the same as in Ref. [4], and is given as

$$F_{\rm el}(q^2) = \int dx d^2k_\perp \frac{M_0}{4x(1-x)}\sqrt{\frac{M_0}{M_0'}}\left[1+\frac{(1-x)\mathbf{k}_\perp\cdot\mathbf{q}_\perp}{k_\perp^2+M^2}\right] \Phi_\pi(x,\mathbf{k}_\perp)\,\Phi_\pi(x,\mathbf{k}'_\perp)\ , \tag{14}$$

where $\mathbf{k}'_\perp = \mathbf{k}_\perp + (1-x)\mathbf{q}_\perp$ and the square free mass $M'^2_0 = ({k'_\perp}^2+m^2)/x(1-x)$. The form factor is evaluated in the Breit frame, where $q^2 = q^\mu q_\mu = -(\mathbf{q}_\perp)^2 = -Q^2$. The resulting q^2 dependence is displayed in Ref. [4]. The pion mean square radius is

$$r_\pi^2 = 6\frac{d}{dq^2}F_{\rm el}(q^2). \tag{15}$$

The previous results for f_π are modified, because the probability of the current $q\bar{q}$ pair is less than unity. The result is

$$f_\pi = \frac{M\sqrt{N_c}}{4\pi^{\frac{3}{2}}}\int\frac{dxd^2k_\perp}{x(1-x)}\frac{\Phi_\pi(x,k_\perp)}{\sqrt{M_0}}\sqrt{\eta}. \tag{16}$$

The value of η will be extracted from the measured value of f_π and this equation.

We next discuss our model in comparison with other models of the pion wave function in the null plane. Phenomenology can be a useful step in allowing us to understand the aspects that a basic theory would need to reproduce. The models of Refs. [6–8,16,17] use constituent quarks, without taking their internal structure into account. QCD sum rules [19] can be used to study quark distribution functions which are integrals of $\Phi_\pi(x,\mathbf{k}_\perp)$ over $d^2k_\perp$. But the present approach is aimed at examining the $k_\perp$ dependence. The model of Ref. [14] considers the structure of the constituent quark in the null-plane framework of the proton wave function. This model is consistent with the general picture used in our approach when dealing with the constituent quark.

To close our discussion, we note that our evaluation of the pion structure function corresponds to an evaluation at some unknown momentum transfer scale (Q_π^2). The idea is that perturbative evolution can be used to obtain the pion distribution at values of Q^2 greater than Q_π^2. Typical values are $Q_\pi^2 \approx 1$ GeV^2 [20] if only the minimal quark configurations are used. We will present results for three different values of Q_π: 0.5, 1, and 1.5 GeV.

III. NUMERICAL RESULTS

The numerical calculations are performed with the following set of nonrelativistic wave functions: (i) Gaussian, in which the main characteristic is confinement, (ii) hydrogen atom that mimics one-gluon exchange at short distances, and (iii) the pion wave-function model of Ref. [13] which has the (iterated) one-gluon exchange and confinement.

The wave function in the null plane is constructed from the nonrelativistic ones according to the rules given in the last section. In the pion model of Ref. [13] the quark mass is 220 MeV. We will allow some variation of M in the hydrogen and Gaussian models, using also $M=$ 300 MeV to explore the mass dependence of the structure function. The structure function is calculated with Eq. (10), once the probability of the $q\bar{q}$ component of the pion wave function η is obtained from f_π [Eq. (16)]. The electromagnetic form factor of the pion and the charge radius are obtained from Eqs. (14) and (15).

The hydrogen-atom and Gaussian wave-function models are obtained from the nonrelativistic radius and in our calculations we use the value of 0.195 fm as given by Ref. [13]. This value is chosen to allow the comparison of the results of the phenomenological models to those obtained from Ref. [13]. This is a somewhat arbitrary choice, since a range of values about 0.195 fm would lead to rather similar spectra.

In Table I, we show the results for the hydrogen and Gaussian models for different quark masses. The value of η is extracted from Eq. (16), where $f_\pi^{\rm expt} = 93$ MeV. The computed value of f_π decreases with increasing quark mass M. Within such models the $q\bar{q}$ probability of about 30% is reached only for M above 300 MeV or core radius smaller than 0.4 fm. The results show quark cores somewhat smaller than the observed pion radius $r_\pi^{\rm expt} = 0.66$ fm. This is reasonable, since in our model the charge

TABLE I. r_π (fm) and η for different models. The nonrelativistic radius is 0.195 fm for each case. The pion model of Ref. [11] ($M = 220$ MeV) and using Ref. [4] gives $r_\pi = 0.456$ fm.

Model	H atom		Gaussian	
M (MeV)	r_π (Ref. [4])	η	r_π (Ref. [4])	η
220	0.463	0.561	0.476	0.741
300	0.408	0.356	0.422	0.476

density of the constituent quark is that of a pointlike object.

Next we turn to computations of the valence structure function of the pion. We wish to compare our results with the parametrization of the experimental data of Ref. [21], at the scale of $Q^2_{\rm expt} = 4\ \mathrm{GeV}^2$. The nonperturbative scale of the pion (Q_π) must be defined to relate our low Q^2 treatment to the data. We choose $Q_\pi \approx 1$ GeV as a reasonable hadronic scale, and allow some variation around this value. We use the first-order Alterelli-Parisi equation [22] to evolve the valence quark structure function $q_v(x, Q^2)$ from the pion scale to the experimental scale. For the purpose of completeness, the formulas for the first-order QCD evolution for the nth moment of q^v_n at the scale Q^2_π to $Q^2_{\rm expt} = 4\ \mathrm{GeV}^2$ are given below:

$$q^v_n(Q^2_{\rm expt}) = q^v_n(Q^2_\pi)\left(\frac{\alpha(Q^2_\pi)}{\alpha(Q^2_{\rm expt})}\right)^{-S_n},$$

$$S_n = \frac{6}{33-2N_F}\,\frac{4}{3}\left(-\frac{1}{2}+\frac{1}{(n+1)(n+2)}-2\sum_{J=1}^{n+1}\frac{1}{J}\right),$$

$$\alpha(Q^2) = \frac{6}{33-2N_F}\,\frac{1}{\ln\frac{Q^2}{\Lambda^2}}, \tag{17}$$

where $\Lambda = 200$ MeV and $N_F = 3$.

The results of QCD evolution in first order are shown in Fig. 3 for the hydrogen-atom model parametrized with $M = 300$ MeV. The values of Q_π of 0.5 and 1.5 GeV are used for comparison. First, note that, even without evolution, Eq. (10) produces a peak at small x without evolution; this is a new feature that Eq. (8) does not have. Clearly, this is an important feature needed to reproduce the experimental data with values of Q_π not extremely small. The effect of the evolution is considerable but the overall behavior of the valence structure function with x comes from Eq. (10). Here the scale of 0.5 GeV/c for the pion is favored by the experimental data as represented by the structure function of Ref. [21]. (That function is very similar to the more recent fit of Ref. [23].)

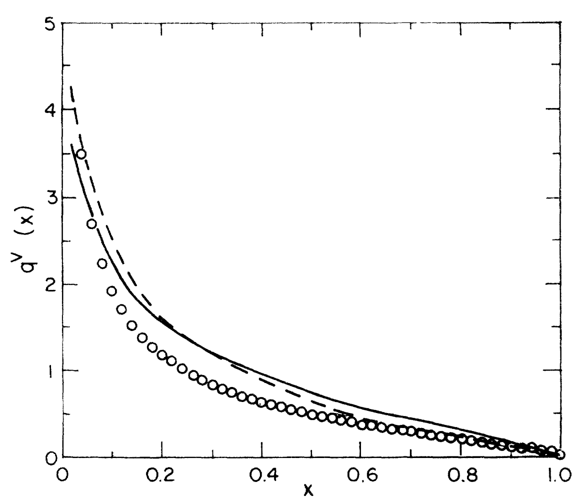

FIG. 4. Effect of the variation of the constituent quark mass in the valence structure function. Hydrogen-atom model, M= 220 MeV (solid line) and 300 MeV (dashed line); $Q_\pi = 0.5$ GeV. Distribution function of Ref. [21] (circles).

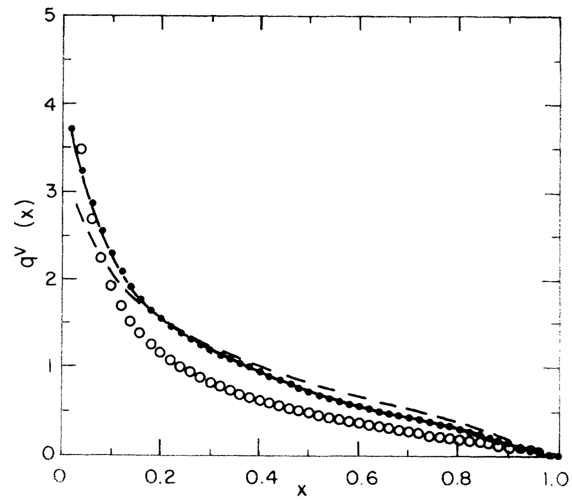

FIG. 5. Model dependence of the valence structure function of the pion. Calculation at the pion scale of $Q_\pi = 0.5$ GeV, evoluted to 2 GeV using first-order QCD evolution. Hydrogen-atom model (solid line), Gaussian model (dashed line), and Ref. [13] (dotted line) with M= 220 MeV. Distribution function of Ref. [21] (circles).

In Fig. 4, the effect of the modification of M is shown for the hydrogen model for $Q_\pi = 0.5$ GeV. The constituent quark mass is a crucial parameter in the null-plane phenomenology, because it defines the change from the instant-form to the null-plane coordinates. So it is important to investigate the effect of mass variations. The change of M from 300 to 220 MeV reduces the structure function at small x. Because η varies inversely as the mass (Table I), the small mass case is dominated by the part of structure function that arises from the $\eta\delta(1-x)$ term of $P(x)$. In the limit of $\eta = 1$, Eq. (10) is reduced to Eq. (8), which does not have a peak at small x.

The model dependence of the pion valence structure function is studied in Fig. 5 with $Q_\pi = 0.5$ GeV and $M = 220$ MeV. The differences between the models are small but Ref. [13] and the hydrogen-atom models are a bit closer to the data. The differences are mainly due to the differences in the value of η.

IV. SUMMARY

The diagrammatic approach is applied to construct the unpolarized deep-inelastic valence structure function of the pion. The formulas are the same as also obtained from Hamiltonian front-form dynamics.

We generalized the previous model [4] to account for the structure of the constituent quark: a current quark surrounded by a cloud of partons. Then the valence structure function takes the convolution form of Eq. (10) of the bound constituent $q\bar{q}$ pair. This expression contains the $\delta(1-x)$ which carries the probability η of having only a current $q\bar{q}$ component in the pion wave function and another part $\hat{P}$ that accounts for the effects caused by momentum sharing (recoil effect) between the current quark and the cloud. At this stage we appeal to simplicity and choose $\hat{P}$ to be constant. The value of η is obtained from the experimental value of f_π. For $\eta < 1$, the quark-core radius is somewhat smaller than the experimental one.

We compare our computed valence structure function of the pion for different models (Ref. [13], Gaussian and hydrogen atom) of the $q - \bar{q}$ bound pair and with a parametrization [21] of the experimental data. The results obtained without including the structure of the constituent quark do not show the qualitative behavior of the data as a function of x. Once the effect of the recoil is introduced the peak at small x is seen for all the models.

Two quantities are important in determining the precise numerical values of the structure function: (i) the constituent quark mass and (ii) the pion scale Q_π. The first one is related to the value of η and the second one to the QCD evolution to the experimental scale. We observed that the data indicate that for values of M about 300 MeV, $Q_\pi \approx 0.5$ GeV is preferred. But our main point is that including effects of the structure of the constituent quark is necessary to obtain the qualitative features of the valence quark distribution function in light-front phenomenologies.

ACKNOWLEDGMENTS

We acknowledge useful discussions with L. L. Frankfurt and M. I. Strikman. T.F. thanks the Theoretical Physics Group at the University of Washington for the warm hospitality and stimulating environment, where this work was developed. This work was supported in part by the Conselho Nacional de Desenvolvimento Científico e Tecnológico - CNPq, Fundação de Amparo à Pesquisa do Estado de São Paulo-FAPESP, Brazil and the U.S. Department of Energy.

APPENDIX

The evaluation of the quark-box diagram for deep-inelastic scattering yields the structure tensor

$$W^{\mu\nu} = (2\pi)^{-1} N_c \sum_{ss'} \mathrm{tr}\Big[u_s(k')\bar{u}_s(k')(ie)\left(\frac{1}{6}+\frac{\tau_3}{2}\right)\gamma^\mu \frac{\not{k}-\not{p}_\pi+M}{(k-p_\pi)^2-M^2+i\epsilon}\gamma^5 \frac{M}{f_\pi}\tau_i \times v_{s'}(-k)\bar{v}_{s'}(-k)\gamma^5\frac{M}{f\pi}\tau_i \frac{\not{k}-\not{p}_\pi+M}{(k-p_\pi)^2-M^2+i\epsilon}(-ie)\left(\frac{1}{6}+\frac{\tau_3}{2}\right)\Big] , \tag{A1}$$

where e is the proton charge, N_c is the number of colors (3), q^μ is the photon momentum, p^μ_π is the pion initial momentum, k^μ is the momentum of the spectator quark, and $k'^\mu = k^\mu - p^\mu_\pi + q^\mu$. The trace is taken over the isospin space. We introduce the quark phase space factors and integrate to obtain

$$W^{\mu\nu} = -(2\pi)^{-1} e^2 N_c \int \frac{d^3k}{(2\pi)^3}\frac{d^3k'}{(2\pi)^3}(2\pi)^4\delta^4(k'-k+p_\pi-q)\frac{M}{k^0}\,\frac{M}{k'^0}\,\frac{M^2}{f_\pi^2} \times \mathrm{tr}\left\{\frac{\not{k}'+M}{2M}\gamma^u\left(\frac{1}{6}+\frac{\tau_3}{2}\right)\frac{\not{k}-\not{p}_\pi+M}{(k-p_\pi)^2-M^2+i\epsilon}\gamma^5\tau_i\frac{\not{k}+M}{2M}\gamma^5\frac{\not{k}-\not{p}_\pi+M}{(k-p_\pi)^2-M^2+i\epsilon}\gamma^\nu\left(\frac{1}{6}+\frac{\tau_3}{2}\right)\right\} . \tag{A2}$$

This can be simplified to

$$W^{\mu\nu} = (2\pi)^{-1}\mathrm{Re}\left\{4N_c e^2\frac{5}{9}\frac{M^2}{f_\pi^2}\int\frac{d^4k}{(2\pi)^4}\frac{\mathrm{tr}(\not{k}'+M)\gamma^u(\not{k}-p_\pi+M)\gamma^5(\not{k}+M)\gamma^5(\not{k}-\not{p}_\pi+M)\gamma^\nu}{(k'^2-M^2+i\epsilon)[(k-p_\pi)^2-M^2+i\epsilon]^2(k^2-M^2+i\epsilon)}\right\} . \tag{A3}$$

The deep-inelastic limit of Eq. (A3) is obtained from the pole contribution of

$$\lim_{q^-\to\infty}\frac{1}{k'^2-M^2+i\epsilon} = -\frac{i\pi}{q^-}\delta(k^+-p^+_\pi+q^+) . \tag{A4}$$

Substituting Eq. (A4) in (A3) we obtain

$$W^{\mu\nu} = \mathrm{Im}\left\{2N_c e^2\frac{5}{9}\frac{M^2}{f_\pi^2}\int\frac{d^4k}{(2\pi)^4}\,\frac{\delta(k^+-p^+_\pi+q^+)}{q^-}\,\frac{\mathrm{tr}(-\not{k}+M)(\not{k}-\not{p}_\pi+m)\gamma^\mu\gamma^\lambda q_\lambda\gamma^\nu(\not{k}-\not{p}_\pi+M)}{(k^2-M^2+i\epsilon)[(k-p_\pi)^2-M^2+i\epsilon]^2}\right\} . \tag{A5}$$

In Eq. (A5) only the term $\gamma^+ q^-$ survives in the deep-inelastic limit. Inserting the identity

$$\gamma^\mu\gamma^\lambda\gamma^\nu = S^{\mu\lambda\nu\sigma}\gamma_\sigma - i\epsilon^{\mu\lambda\nu\sigma}\gamma_\sigma\gamma^5$$

and $S^{\mu\lambda\nu\sigma} = g^{\mu\lambda}g^{\nu\sigma} + g^{\mu\sigma}g^{\lambda\nu} - g^{\mu\nu}g^{\lambda\sigma}$ in Eq. (A5), Eq. (2) is obtained for the unpolarized process.

[1] S. Weinberg, Phys. Rev. **150**, 1313 (1966); L. Susskind, *ibid.* **165**, 1535 (1968); **165**, 1547 (1968); K. Bardakci and M.B. Halpern, Phys. Rev. **176**, 1686 (1968); D.E. Soper, Ph.D thesis, Stanford University, 1971; H. Leutwyler and J. Stern, Ann. Phys. (N.Y.) **112**, 94 (1978).

[2] H. Leutwyler, Nucl. Phys. **B76**, 413 (1974); M.V. Terent'ev, Yad. Fiz. **24**, 207 (1976) [Sov. J. Nucl. Phys. **24**, 106 (1976)]; B.L.G. Bakker, L.A. Kondratyuk, and M.V. Terent'ev, Nucl. Phys. **B158**, 497 (1979); L.A. Kondratyuk and M.V. Terent'ev, Yad. Fiz. **31**, 1087 (1980) [Sov. J. Nucl. Phys. **31**, 561 (1980)].

[3] L.L. Frankfurt and M.I. Strikman, Nucl. Phys. **B148**, 107 (1979); Phys. Rep. **76**, 215 (1981).

[4] T. Frederico and G.A. Miller, Phys. Rev. D **45**, 4207 (1992).

[5] Good operators are characterized by having matrix elements between hadronic states of momentum P that are of the order of P as P approaches infinity. Such operators do not connect the bare vacuum to pair states if P is large. R. Dashen and M. Gell-Mann, *Proceedings of the 3rd Coral Gables Conference on Symmetry Principles at High-Energy* (Freeman, San Francisco, 1966); S. Fubini, G. Segré, and D. Walecka, Ann. Phys. **39**, 381 (1966); V. de Alfaro, S. Fubini, G. Furlan, and C. Rossetti, *Currents in Hadron Physics* (North-Holland, Amsterdam, 1973).

[6] P.L. Chung, F. Coester, and W.N. Polyzou, Phys. Lett. B **205**, 545 (1988); P.L. Chung, F. Coester, B.D. Keister, and W.N. Polyzou, Phys. Rev. C **37**, 2000 (1988).

[7] C.R. Ji and S. Cotanch, Phys. Rev. D **21**, 2319 (1990); S. Cotanch (private communication).

[8] C.R. Ji, P.L. Chung, and S. Cotanch, Phys. Rev. D **45**, 4214 (1992); W. Jaus, *ibid.* **44**, 2851 (1991); B.-Q. Ma, Z. Phys. A **345**, 321 (1993).

[9] U. Oelfke, P.U. Sauer, and F. Coester, Nucl. Phys. **A518**, 593 (1990).

[10] G.P. Lepage and S.J. Brodsky, Phys. Rev. D **22**, 2175 (1980).

[11] G.P. Lepage, S.J. Brodsky, T. Huang, and P.B. Mackenzie, in *Particles and Fields—2*, Proceedings of the Banff Summer Institute, Banff, Alberta, 1981, edited by A.Z. Capri and A.N. Kamal (Plenum, New York, 1983), p.83.

[12] V. Bernard and U.G. Meissner, Phys. Rev. Lett. **61**, 2296 (1988).

[13] S. Godfrey and N. Isgur, Phys. Rev. D **32**, 189 (1985).

[14] Z. Dziembowski and J. Franklin, J. Phys. **17**, 213 (1991).

[15] C. Itzykson and J.B. Zuber, *Quantum Field Theory* (McGraw-Hill, New York, 1980).

[16] Z. Dziembowski and L. Mankiewicz, Phys. Rev. Lett. **58**, 2175 (1987).

[17] Z. Dziembowski, Phys. Rev. D **37**, 768 (1988); **37**, 778 (1988).

[18] J.D. Bjorken and S.D. Drell, *Relativistic Quantum Fields* (McGraw-Hill, New York, 1965).

[19] V.L. Chernyak and A.R. Zhitnitskii, Phys. Rep. **112**, 173 (1984).

[20] R.L. Jaffe and G.G. Ross, Phys. Lett. **93B**, 313 (1980).

[21] J.F. Owens, Phys. Rev. D **30**, 943 (1984).

[22] G. Altarelli and G. Parisi, Nucl. Phys. **B126**, 298 (1984); Particle Data Group, J.J. Hernandez *et al.*, Phys. Lett. B **239**, 1 (1990).

[23] P.J. Sutton, A.D. Martin, R.G. Roberts, and W.J. Stirling, Phys. Rev. D **45**, 2349 (1992).